IEEE Access
Multidisciplinary | Rapid Review | Open Access Journal

SPECIAL SECTION ON GNSS, LOCALIZATION, AND NAVIGATION TECHNOLOGIES

Received January 12, 2018, accepted February 3, 2018, date of publication February 8, 2018, date of current version March 15, 2018.

Digital Object Identifier 10.1109/ACCESS.2018.2803742

Turbo Receiver Channel Estimation for GFDM-Based Cognitive Radio Networks

ZHENYU NA[1], (Member, IEEE), ZHENG PAN[1], MUDI XIONG[1], XIN LIU[2], (Member, IEEE), WEIDANG LU[3], (Member, IEEE), YONGJIAN WANG[4], AND LISHENG FAN[5]

[1]School of Information Science and Technology, Dalian Maritime University, Dalian 116026, China
[2]School of Information and Communication Engineering, Dalian University of Technology, Dalian 116024, China
[3]College of Information Engineering, Zhejiang University of Technology, Hangzhou 310058, China
[4]Laboratory of National Internet Emergency Center, Beijing 100029, China
[5]School of Computer Science and Educational Software, Guangzhou University, China

Corresponding author: Mudi Xiong (xiongmudi@dlmu.edu.cn) and Xin Liu (liuxinstar1984@dlut.edu.cn)

This work was supported in part by the National Natural Science Foundation of China under Grant 61301131 and Grant 61601221, in part by the Natural Science Foundations of Jiangsu Province under Grant BK20140828, in part by the China Postdoctoral Science Foundation under Grant 2015M580425, and in part the Fundamental Research Funds for the Central Universities under Grant 3132016347 and Grant DUT16RC(3)045.

ABSTRACT Generalized frequency division multiplexing (GFDM) is a promising candidate for 5G waveforms because of its flexibility to meet the requirements of different scenarios and applications. Compared with the orthogonal frequency division multiplexing, the lower out-of-band radiation and higher spectrum efficiency make GFDM the qualified waveform solution for cognitive radio (CR). In CR networks, channel estimation is the necessity and premise to guarantee reliable spectrum sensing. Because of the block modulation structure for GFDM, conventional channel estimation algorithm cannot be applied to GFDM directly. Also, the feedback information in channel decoding is not fully utilized by the conventional algorithm. To solve these problems, in this paper, a modified turbo receiver is designed to utilize the feedback information for channel estimation. The modulator for the pilot insertion is also improved to make pilots orthogonal to data subcarriers. Based on the modified turbo receiver, an iterative channel estimation strategy combined with threshold control is proposed to cope with the noise enhancement. The symbols rebuilt for the iterative channel estimation are verified that only the credible symbols can be retained for the next iteration. Simulation results demonstrate that the proposed channel estimation method has the better bit error rate and mean-squared error performances over Rayleigh fading channel compared with the conventional algorithm.

INDEX TERMS Cognitive radio, GFDM, channel estimation, turbo codes, threshold control.

I. INTRODUCTION

The Internet and mobile communication networks have experienced an explosive growth in last decade. As the web-based applications, online music, videos, transactions via mobile Internet and massive Internet of Things (IoT) connections grow drastically, huge amounts of wireless data greedily occupy bandwidth and spectrum resources. How to deal with spectrum scarcity is the primary problem in wireless communications. Cognitive Radio (CR) is one of the most promising technologies to solve spectrum scarcity. By sensing the ''spectrum hole'' of the primary user (PU), CR enables the opportunistic spectrum access for the secondary user (SU). Thus, CR is a high-efficiency way to enhance spectrum utilization [1], [2].

In recent years, the research on CR mainly focus on spectrum sensing, resource allocation, cognitive radio network cloud as shown in Fig.1, and signal modulations for CR physical layer [3]–[8]. As the key air interface technology of the 4th Generation (4G) mobile communications, Orthogonal Frequency Division Multiplexing (OFDM) has been comprehensively investigated. OFDM has always been considered as the optimal technique for CR physical layer because of its flexibility in both subcarrier selection and transmission power adjustment, robustness against multipath channel and easy hardware implementation [9], [10]. Either to detect the unoccupied spectrum or to improve the utilization of the occupied spectrum is the effective way to improve the spectrum utilization. Although OFDM is qualified for CR, there are some shortcomings that make OFDM difficult to meet the spectrum requirements of different applications in the future 5G scenarios. Firstly, each OFDM symbol has one cyclic prefix (CP) that greatly decreases the spectrum

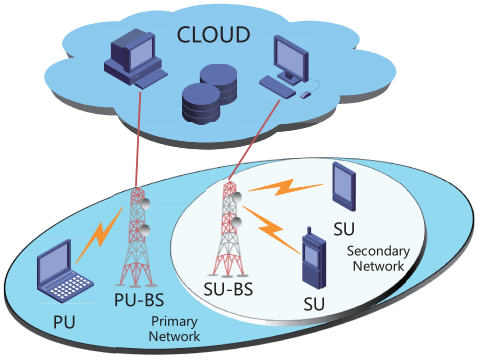

FIGURE 1. Cognitive radio networks cloud.

efficiency. Secondly, since OFDM has an exorbitant Out-of-Band (OoB) radiation, the wider guard interval (GI) is necessary leading to that the dynamic spectrum access can't be implemented easily. Finally, because OFDM system is highly sensitive to the loss of synchronization, its applications to 5G wireless scenarios such as the Internet of Things (IoT), Machine-Type Communications (MTC) and massive connections are restricted.

Oriented to the forthcoming 5G era, several advanced physical layer technologies have been proposed to overcome the flaws of OFDM. As the candidate waveforms for 5G, e.g., both the Filter Bank Multicarrier (FBMC) and Generalized Frequency Division Multiplexing (GFDM) are proved to be suitable for CR [11]–[13]. In FBMC system, the OoB radiation is highly reduced by the well-designed pulse shaping filter. Since the low OoB achieves at a cost of very long filter impulse response, FBMC is not suitable for the low-latency applications. Besides, the Offset Quadrature Amplitude Modulation (OQAM) is preferred by FBMC. In this case, the combination of OQAM-FBMC with Multiple-Input Multiple-Output (MIMO) will complicate the receiver design [14]–[16]. GFDM is a generalized form of OFDM. Different from OFDM, GFDM modulation adopts the two-dimensional time-frequency data block, and each data block comprises several subsymbols and subcarriers. The time-frequency structure of GFDM data blocks can flexibly adapt to the different applications and scenarios. Due to only one Cyclic Prefix (CP) added to the entire GFDM data block, the spectrum efficiency of GFDM is higher than OFDM [10], [16], [17]. GFDM inherits most advantages of OFDM, such as easy combination with MIMO and easy hardware implementation by the Fast Fourier Transformation (FFT) and Inverse FFT (IFFT) [18]. Since the OoB radiation to the adjacent frequency band is extremely low, GFDM is more qualified for the CR physical layer. The applications of GFDM to CR have already been studied widely. As expected, the performance of GFDM in CR is better than OFDM [11], [12]. The performance comparison between FBMC and GFDM in the context of CR is out of scope of this paper.

As one of the key physical layer techniques, channel estimation is essential for reliable communications. In OFDM systems, the traditional channel estimation based on channel frequency response (CFR) can be divided into three categories: blind channel estimation, preamble based channel estimation and pilot based channel estimation. The blind channel estimation does not need any priori information of data symbols at the receiver. Compared with other estimation methods, the blind channel estimation has the advantage of high spectrum efficiency. But most of existing blind estimation methods require a sufficient amount of data blocks to build a reliable sample covariance matrix. The preamble based channel estimation uses preamble training symbols to estimate CFR. Then, the subsequent data symbols are equalized by using the estimated CFR. The main problem of this type of methods lies in the error propagation which can be solved by increasing the number of inserted training symbols periodically. As a result, the preamble based channel estimation is converted into the pilot based channel estimation with the advantages of low complexity and high reliability [9], [19], [20].

The pilot based channel estimation has been extensively studied in OFDM systems. However, traditional pilot based channel estimation methods can't be applied to GFDM systems directly mainly because of the block-based modulation of GFDM. In [21], a common idea to separate the pilot from data symbols is used for the channel estimation in GFDM-based system, but the interference pre-cancelation is based on the prior knowledge of both pilot and data symbols available at the transmitter. Moreover, this method is only simulated in the condition of frequency flat-fading channel so that it is not suitable for the frequency-selective fading channel and broadband communications. In [18] and [22], the existing channel estimation methods in OFDM systems, which use multiple pilots in each pilot subcarrier, are introduced into GFDM system, and their performance is evaluated. However, the received reference symbols are often influenced by data symbols due to the Inter-Carrier Interference (ICI) from the non-orthogonality between subcarriers. In order to eliminate ICI, in [23], an interference-free pilot insertion technique is proposed. By redesigning GFDM modulator, the pilots can be modulated to the reserved frequency bins orthogonal to the data symbols. At a small cost of OoB radiation, the interference from data symbols can be completely canceled. In their works, the parallel concatenated convolutional codes are used to improve the bit error rate (BER) performance, but the feedback information from iterative decoder is underutilized. In the OFDM system with iterative decoder, the iterative channel estimation approaches are widely investigated. The core vision of iterative channel estimation is to improve the accuracy of channel estimation by using the soft information from iterative decoder [24]–[30]. Based on these researches, we have proposed a Turbo receiver channel estimation method for GFDM-based CR networks in this paper. The main contributions of this paper are summarized as follows:

- We design a Turbo receiver channel estimator for GFDM-based CR networks. The feedback soft

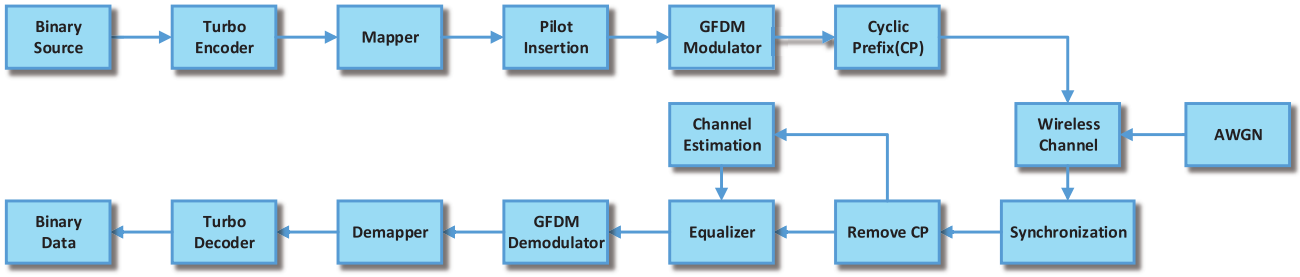

FIGURE 2. Basic block diagram of the GFDM transceiver.

information in iterative decoding process is utilized to ameliorate channel estimation. In the basic Turbo receiver, the feedback soft information is only used for soft demapper. In this paper, we use the soft information to rebuild the data symbols which are regarded as known pilots for channel estimation in the next iteration.

- A threshold control strategy for the Turbo receiver channel estimation is proposed to deal with noise enhancement. In the condition of low Signal-to-Noise Ratio (SNR) environment, the feedback soft information is unauthentic. The use of the soft information to rebuild data symbols not only intensifies the noise, but also deteriorates the system performance. The threshold control strategy can judge whether the rebuilt data symbols are credible. Based on this strategy, the feedback information can be used credibly and the performance of the iterative channel estimation can be improved.
- We build an improved modulator for GFDM pilot insertion to make the pilots free from the influence of data. By making the pilots orthogonal to the data subsymbols on the pilot subcarriers, the pilots can be separated from the received signal without any interference from the data symbols. Combined with the improved modulator, the proposed Turbo receiver channel estimation can be effectively improved.

The rest of the paper is organized as follows. The basic GFDM system model is described in Section II where the implementation of the transmitter and receiver of GFDM system is described. The pilot insertion and channel estimation are introduced in Section III. The Turbo receiver channel estimation for GFDM-based CR networks and the threshold control strategy are expounded in Section IV. The simulation results are demonstrated and discussed in Section V. Finally, Section VI concludes this paper.

II. GFDM SYSTEM MODEL

The Turbo-coded GFDM system under consideration is shown in Fig. 2. After coded by Turbo encoder, the coded binary source $\vec{b}_c$ is mapped by a mapper, e.g. Phase Shift Keying (PSK) or Quadrature Amplitude Keying (QAM). After μ-order modulation, the coded bits in $\vec{b}_c$ are mapped into 2^{μ}-valued complex constellation symbols. The mapped

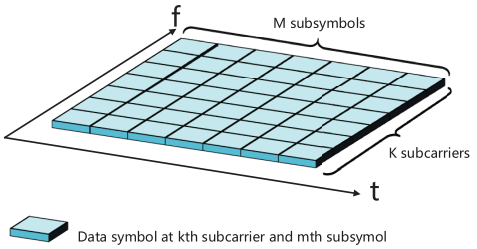

FIGURE 3. Block structure of GFDM system.

vector $\vec{s}$ contains $N = MK$ symbols. K is the number of subcarriers and M is the number of subsymbols. The individual entries of the vector

$$\vec{s} = (s_{0,0}, s_{1,0}, \cdots, s_{K-1,0}, s_{0,1}, \cdots, s_{K-1,M-1})^T$$

are donated by $s_{k,m}$ which are corresponding to the transmission data symbol on kth subcarrier and in the mth subsymbol of GFDM data block. After serial-to-parallel conversion, $\vec{s}$ is reshaped into a $K \times M$ data block given below

$$S = \begin{bmatrix} s_{0,0} & \cdots & s_{0,M-1} \\ \vdots & \ddots & \vdots \\ s_{K-1,0} & \cdots & s_{K-1,M-1}. \end{bmatrix} \quad (1)$$

The structure of (1) is shown in Fig.3. In GFDM modulation, each data symbol $s_{k,m}$ is pulse-shaped by a filter impulse response

$$g_{k,m}[n] = g[(n - mK)modN] \cdot exp[-j2\pi \frac{k}{K} n], \quad (2)$$

where n denotes the sampling index, $g_{k,m}[n]$ is derived from the time and frequency shifting of the prototype filter $g[n]$. Formally, the transmission sample of GFDM [10] is given by

$$x[n] = \sum_{k=0}^{K-1} \sum_{m=0}^{M-1} g_{k,m}[n] s_{k,m}, \quad (3)$$

where $n = 0, \cdots, N-1$. The GFDM modulation process can be rewritten into a matrix-vector form as

$$\vec{x} = A\vec{s}. \quad (4)$$

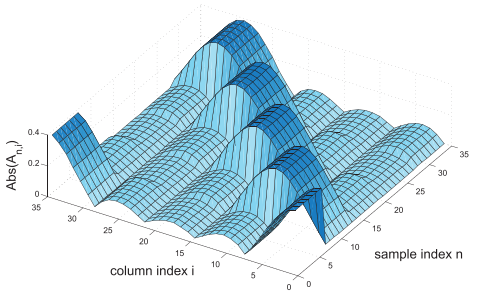

FIGURE 4. Illustration of GFDM transmission matrix for N=35, K=7, M=5 and the roll-off factor of RC filter is 0.3.

The transmission matrix $\boldsymbol{A}$ is a $KM \times KM$ matrix with the structure as

$$\boldsymbol{A} = (\vec{g}_{0,0}, \cdots, \vec{g}_{K-1,0}, \vec{g}_{0,1}, \cdots, \vec{g}_{K-1,M-1}). \tag{5}$$

where $g_{k,m} = (g_{k,m}[0], g_{k,m}[1], \cdots, g_{k,m}[N-1])^T$. All the modulation operations can be integrated into a transmission matrix $\boldsymbol{A}$. The illustration of the transmission matrix is shown in Fig. 4.

The modulation process in frequency domain which is derived from formula (2) and (3) is given by

$$\vec{x} = \boldsymbol{W}_N^H \sum_{k=0}^{K-1} \boldsymbol{C}_f^{(k)} \Gamma_f^{(L)} \boldsymbol{R}_f^{(L)} \boldsymbol{W}_M \vec{s}_k, \tag{6}$$

where $\vec{d}_k$ represents the data symbols on the kth sub-carrier. The data symbols are transformed first into frequency domain through the $M \times M$ Discrete Fourier Transform (DFT) matrix $\boldsymbol{W}_M = \{e^{-j2\pi \frac{ij}{M}}\}_{M\times M}$, where $i = 0, \cdots, M-1$ and $j = 0, \cdots M-1$. $\boldsymbol{R}_f^{(L)} = (\boldsymbol{I}_M \boldsymbol{I}_M \cdots \boldsymbol{I}_M)^T$ is the repetition matrix, which is a concatenation of L identity matrices $\boldsymbol{I}_M$ with the size of $M \times M$. This repetition operation corresponds to the upsampling in time domain with a factor L. Subsequently, each subcarrier is filtered in frequency domain. The filter matrix $\Gamma_f^{(L)}$ is a diagonal matrix in which $\boldsymbol{W}_{LM} g^{(L)}$ is on its diagonal. $g^{(L)}$ can be reduced to LM samples by down-sampling with the factor N/L. Finally, the kth subcarrier is up-converted to its corresponding frequency using a cyclic matrix $C_f^{(L)}$, which can be constructed according to

$$\begin{aligned} \boldsymbol{C}_f^{(0)} &= \begin{pmatrix} \boldsymbol{I}_{LM/2} & \boldsymbol{0}_{LM/2} & \cdots & \boldsymbol{0}_{LM/2} & \boldsymbol{0}_{LM/2} \\ \boldsymbol{0}_{LM/2} & \boldsymbol{0}_{LM/2} & \cdots & \boldsymbol{0}_{LM/2} & \boldsymbol{I}_{LM/2} \end{pmatrix}^T \\ \boldsymbol{C}_f^{(1)} &= \begin{pmatrix} \boldsymbol{0}_{LM/2} & \boldsymbol{I}_{LM/2} & \cdots & \boldsymbol{0}_{LM/2} & \boldsymbol{0}_{LM/2} \\ \boldsymbol{I}_{LM/2} & \boldsymbol{0}_{LM/2} & \cdots & \boldsymbol{0}_{LM/2} & \boldsymbol{0}_{LM/2} \end{pmatrix}^T, \end{aligned} \tag{7}$$

where $\boldsymbol{0}_{LM/2}$ is an $\frac{LM}{2} \times \frac{LM}{2}$ matrix containing only zero elements. The cyclic matrix C_f converts the higher and the lower spectrum components of the subcarrier at the baseband into the components at the passband. Because of the time-frequency structure of GFDM data blocks, the modulation operation can be implemented in both frequency domain and in time domain. Although the time domain modulation has lower complexity [31], we realize the modulation in frequency domain mainly because the channel estimation is performed in frequency domain. Before transmission, CP is added to combat multipath fading and inter block interference (IBI). Compared with OFDM, GFDM adds CP to the entire data block to improve spectrum efficiency. Then, the signal is transmitted over the multi-path wireless channel. For the convenience of analysis, we assume that the received signal is perfectly synchronized in time and frequency. After CP is removed, the received signal can be expressed as

$$\vec{y} = \vec{x} \circledast \vec{h} + \vec{w}, \tag{8}$$

where $\circledast$ denotes the circular convolution operation and $\vec{h}$ denotes the channel impulse response of the frequency selective Rayleigh fading channel. $\vec{h}$ is obtained from the matrix of the normalized power delay profile (PDP). In frequency domain, the observed signal $\vec{Y}$ is expressed as:

$$\vec{Y} = \boldsymbol{H}\vec{X} + \vec{W}, \tag{9}$$

where $\boldsymbol{H} = \boldsymbol{W}^H \vec{h} \boldsymbol{W}$, $\vec{X} = \boldsymbol{W}^H \vec{x}$ and $\vec{W} = \boldsymbol{W}^H \vec{w}$. $\boldsymbol{W}$ denotes the DFT matrix and $\boldsymbol{W}^H$ is the unitary DFT matrix. The Zero-Forcing (ZF) equalizer similiar to that used in OFDM can also be adopted by GFDM. The ZF based channel equalization can be performed as

$$\vec{z} = IDFT\left(\frac{\vec{Y}}{\vec{\breve{H}}}\right), \tag{10}$$

where $\vec{z}$ is the received signal after equalization and $\vec{\breve{H}}$ is the estimated CFR. With the knowledge of noise variance σ_w^2, the minimum mean square error (MMSE) equalization can be employed to combat noise. The MMSE equalization operation is given as:

$$\begin{aligned} \vec{z} &= IDFT(\boldsymbol{Q}\vec{Y}) \\ \boldsymbol{Q} &= (\vec{\breve{H}}^H \vec{\breve{H}} + \sigma_w^2 I_N)^{-1} \vec{\breve{H}}^H, \end{aligned} \tag{11}$$

where I_N denotes the identity matrix. Based on (4), the GFDM demodulation with ZF algorithm can be written as

$$\vec{\hat{s}} = \boldsymbol{A}^{-1}\vec{z}, \tag{12}$$

Similar to the frequency domain GFDM modulation, the implementation of GFDM demodulation can be expressed as

$$\vec{\hat{d}}_k = \boldsymbol{W}_M^H (R^{(L)})^T \Gamma_{RX}^{(L)} (\boldsymbol{C}^{(k)})^T \boldsymbol{W}_N \vec{z}, \tag{13}$$

Finally, the demodulated symbols $\vec{\hat{d}}$ are demapped into a bit sequence which is then sent to Turbo decoder to recover the binary data stream.

III. PILOT INSERTION AND CHANNEL ESTIMATION

The pilots are inserted into the data blocks with a specific interval. As shown in Fig.5, we put only one pilot subsymbol on each pilot subcarrier. The constant enveloped Zadoff-Chu sequence is used as the pilot sequence of the channel estimation for GFDM-based CR networks. In time and frequency

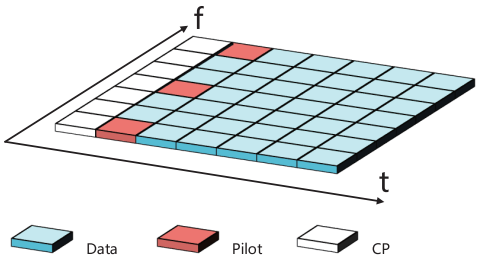

FIGURE 5. Overview of the pilots and data symbols.

domains, since the two-dimensional sequence is constant enveloped, it has the strong ability to combat noise. Besides, the sequence also has good phase characteristics. These two advantages make the Zadoff-Chu sequence widely used in channel estimation. The Zadoff-Chu sequence is given as:

$$u_k = \begin{cases} exp\left(-\frac{j2\pi}{N_p}\right)^{\frac{k^2}{2}+k}, & N_p \text{ is even} \\ exp\left(-\frac{j2\pi}{N_p}\right)^{\frac{k(k+1)}{2}+k}, & N_p \text{ is odd}, \end{cases} \tag{14}$$

where $k = 0, 1, \cdots, N_p - 1$, $N_p = round(\frac{N}{\Delta k})$ denotes the length of pilot sequence and Δk is the spacing between each pilot symbol. In conventional GFDM system, pilot symbols and data symbols are modulated together. Since the pilot subcarriers are non-orthogonal to data subcarriers, the interference between data and pilot symbols appears. In order to eliminate the interference from data symbols, we use an interference-free modulation to make pilot subcarriers orthogonal to data subcarriers. The modulation for data subcarriers is the same as (6), while the modification of (6) for pilot subcarriers is shown as follows:

$$\vec{x}_p = \boldsymbol{W}_N^H \sum_{k=0}^{K-1} \boldsymbol{C}_f^{(k)} \Gamma_f^{(L)} \boldsymbol{R}_f^{(L)} \mathbb{W} \vec{\tilde{s}}_k \tag{15}$$

$$\vec{s} = \vec{\tilde{s}} + \vec{\tilde{s}} \tag{16}$$

$$\mathbb{W} = blkdiag(I_n, \boldsymbol{W}_{M-n}). \tag{17}$$

Here, $\vec{x}_p$ contains the modulated data and the pilot symbols only in the position of pilot subcarriers. $\vec{\tilde{s}}_k$ denotes the subsymbols only on pilot subcarriers and $\vec{\tilde{s}}$ is the subsymbols only on data subcarriers. $\vec{\tilde{s}}_k \circ \vec{\tilde{s}} = \vec{0}_N$, where $\circ$ represents the Hadamard product. Because of (17), the first n subsymbols of pilot subcarriers are isolated from data symbols. The processing of isolation makes the pilots locate at the frequency orthogonal to data subcarriers and keep the pilots away from ICI. An example of signal spectrum for $K = 4$, $M = 20$ is shown in Fig. 6 where the pilots are orthogonal to data and pilot subcarriers. The pilot subcarriers are still non-orthogonal to data subcarriers that means this method of the pilot modulation can achieve a better performance only at a small cost. Based on (6) and (15), the transmission signal can be defined as $\vec{x} = \vec{x}_d + \vec{x}_p$, which $\vec{x}_d$ is the modulated signal

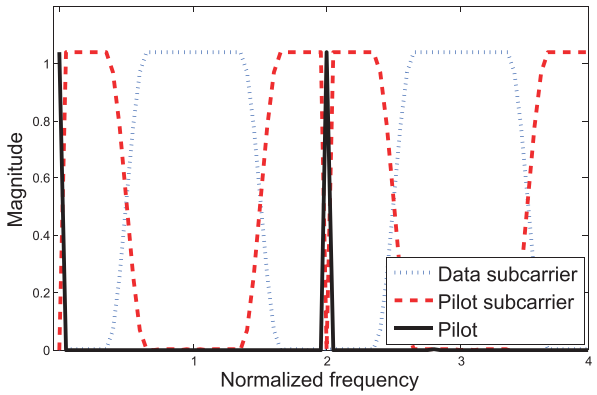

FIGURE 6. Signal spectrum with othorgonal pilots.

of the symbols on data subcarriers. So, for GFDM channel estimation, the observed signal in frequency domain follows:

$$\vec{Y} = \boldsymbol{H}(\vec{X}_d + \vec{X}_p) + \vec{W}, \tag{18}$$

where $\vec{X}_d$ and $\vec{X}_p$ are the symbols on data subcarriers and pilot subcarriers in frequency domain, respectively.

Because of the orthogonality between the pilots and the data symbols, the pilots can be separated from the received signal without the influence from the data symbols. $\boldsymbol{W}_p$ is the separation matrix which performs DFT only on the pilot subcarriers. Every $n + 1$ row of $\boldsymbol{W}_p$ is coming from $\Delta kMn+1$ row of $N \times N$ DFT matrix $\boldsymbol{W}$, where $n = 0, 1, \cdots, N_p - 1$. The reference pilot symbols at the receiver are given as follows:

$$\vec{Y}_{pilot} = \boldsymbol{W}_p \vec{Y} \tag{19}$$

The Least Square (LS) channel estimation to minimize $\|\vec{Y}_{pilot} - \boldsymbol{H}\vec{X}_{pilot}\|^2$ can be expressed as:

$$\vec{\tilde{H}}_{pilot} = \frac{\vec{Y}_{pilot}}{\vec{X}_{pilot}} = \vec{H}_{pilot} + \frac{\vec{W}_{pilot}}{\vec{X}_{pilot}}. \tag{20}$$

Finally, the CFR estimation for all subcarriers can be obtained from:

$$\vec{\tilde{H}} = \boldsymbol{filter}(\vec{\tilde{H}}_{pilot}), \tag{21}$$

where $\boldsymbol{filter}(\bullet)$ denotes the DFT based interpolation filter. By using a priori knowledge of the maximum multipath delay, the estimated impulse response is truncated to reduce interference.

IV. TURBO RECEIVER CHANNEL ESTIMATION

In this section, we will describe the basic structure of Turbo-coded receiver. Based on it, we design a novel Turbo receiver for channel estimation. Subsequently, a threshold control strategy is proposed to improve the performance of the Turbo receiver channel estimation for GFDM-based CR networks.

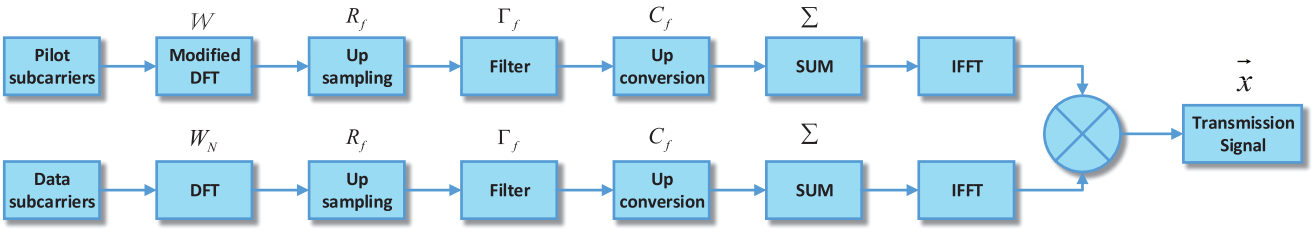

FIGURE 7. Block diagram of GFDM modulation for pilots and data.

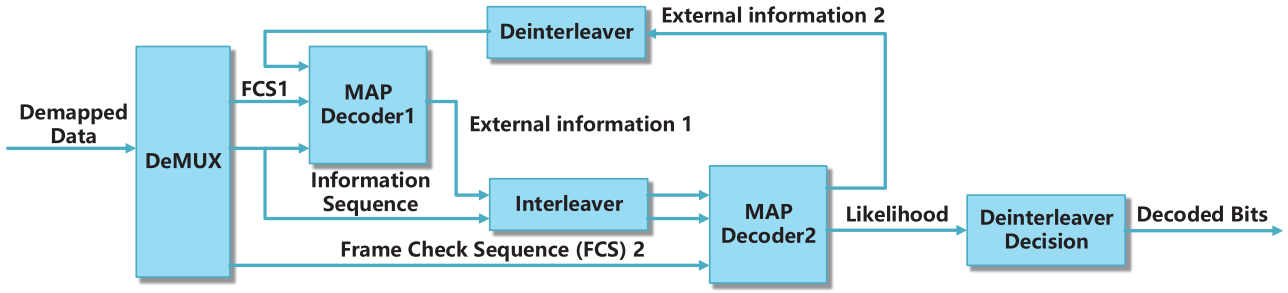

FIGURE 8. Typical structure of Turbo-coded decoder.

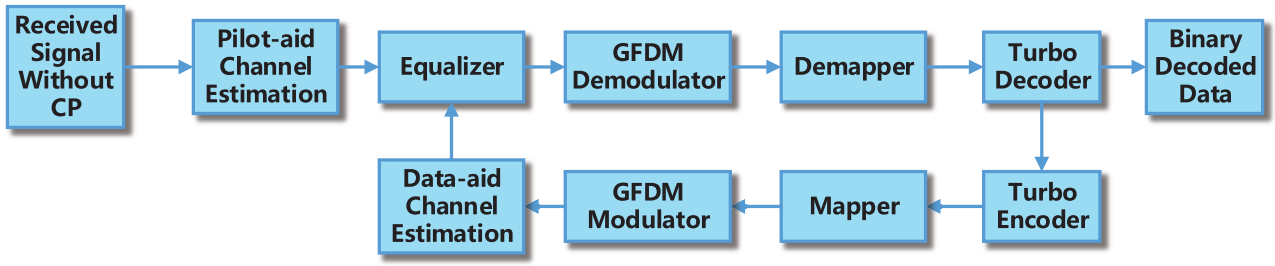

FIGURE 9. Modified Turbo receiver for channel estimation.

A. ITERATIVE CHANNEL ESTIMATION FOR TURBO RECEIVER

After GFDM demodulation and demapping, the demapped binary data stream is decoded by Turbo decoder. The typical structure of Turbo decoder is shown in Fig. 8. The Turbo decoder is composed of two component decoders 1 and 2. They are linked by interleaver and deinterleaver to form a closed-loop feedback. Each component decoder uses the Soft-In-Soft-Out (SISO) and Maximum a Posteriori (MAP) algorithm. The frame check sequence (FCS) and information sequence are demultiplexed from the binary data stream and sent to each MAP decoder. The external information 1 from MAP decoder 1 and the information sequence are sent to MAP decoder 2 after interleaving. The external information 2 is fed back to MAP decoder 1 for the next iteration after deinterleaving. The external information from each MAP decoder becomes stable in the iterative process. The likelihood ratio of each bit is asymptotically close to the maximum likelihood decoding. Finally, the optimal estimation of each bit is obtained from the likelihood ratio by hard decision. In order to utilize the external information fed back in each iteration, we design an improved Turbo receiver for iterative channel estimation.

The block diagram of the Turbo receiver channel estimation for GFDM-based CR networks is shown in Fig. 9. The iterative channel estimation process can be generally divided into three stages.

The first is the pilot-aided initial channel estimation stage. Based on (20) and (21), the received signal without CP is firstly equalized by the estimated CFR.

The next is the data-aided iterative channel estimation stage. In each iteration of the stage, the soft output of the MAP decoder is encoded for the data-aided estimation. The output log-likelihood ratio $L_\alpha(c_k)$ can be transformed into bit probability by the following:

$$P(c_k = 0) = \frac{1}{1 + e^{L_\alpha(c_k)}}$$
$$P(c_k = 1) = \frac{e^{L_\alpha(c_k)}}{1 + e^{L_\alpha(c_k)}} \quad (22)$$

By virtue of random interleaver, the coded bits can be regarded as statistically independent. After QAM or PSK mapping, the symbol probability can be written as the product of (22):

$$P_i(k,m) = P(S_{k,m} = B_i) = \prod_{k=1}^{\mu} P(c_k = b_k), \tag{23}$$

where B_i denotes the modulation symbol homologous to the bit sequence $[b_1, b_2, \cdots, b_\mu]$. Based on the hard mapper, the symbol with the highest probability is selected from the modulation alphabet elements:

$$\hat{S}_{k,m} = \arg\max_{B_i \in \mathcal{B}} \left\{ P(S_{k,m} = B_i) \right\}, \tag{24}$$

where $\mathcal{B} = \{1, 2, \cdots, 2^\mu\}$ is the set of modulation symbols from a 2^μ-valued constellation.

Thus, the rebuilt symbols $\vec{\tilde{X}}_{data}$are regarded as the known pilots for data-aided channel estimation. By applying LS estimation, the estimated CFR can be expressed as:

$$\vec{\tilde{H}}(n) = \begin{cases} \vec{\tilde{H}}_{pilot}(n) & n \in pilot \\ \dfrac{\vec{Y}_{data}(n)}{\vec{\tilde{X}}_{data}(n)} & n \in data. \end{cases} \tag{25}$$

The estimated CFR $\vec{\tilde{H}}$ is used for equalization in the next iteration.

The final stage is performed in the last iteration. The hard decision is carried out to get the final decoded bits.

B. THRESHOLD CONTROL FOR ITERATIVE ESTIMATION

Although the proposed Turbo receiver channel estimation for GFDM can utilize the feedback information, the estimation still suffers from a bias because of the imperfect decoded information. If we perform the equalization by using the CFR which comes from the data-aided estimation directly, the noise will be enhanced and the performance of the proposed channel estimation will deteriorate evidently. Therefore, we propose a threshold control strategy to deal with the noise enhancement. The Mean-Square Error (MSE) of the data-aided LS channel estimation in the position of data symbols can be given as:

$$\begin{aligned} \vec{\tilde{H}}_d &= \vec{H} + \frac{\vec{W}}{\vec{\tilde{X}}} \\ MSE_{data} &= \mathbb{E}[|\vec{H} - \vec{\tilde{H}}_d|^2] \\ &= \frac{\sigma_w^2}{|\vec{\tilde{X}}|^2}. \end{aligned} \tag{26}$$

For the pilot-aided channel estimation, the MSE in the position of data symbols is expressed as

$$\begin{aligned} MSE_{pilot} &= \mathbb{E}[|\vec{H} - \vec{\tilde{H}}_p|^2] \\ &= \mathbb{E}[|\vec{H} - F_{in}(\vec{\tilde{H}}_{pilot} + \frac{W_{pilot}}{\vec{\tilde{H}}_{pilot}})|^2] \\ &= \frac{1}{N} Tr\{R_{hh} - 2Re[F_{in}R_{hp}^H] \\ &\quad + F_{in}(R_{pp} + \frac{\sigma_w^2}{\sigma_x^2}\boldsymbol{I}_{N_p})F_{in}^H\}, \end{aligned} \tag{27}$$

where F_{in} is the interpolation filter matrix.

$$\boldsymbol{filter}(\vec{\tilde{H}}_{pilot}) \triangleq F_{in}\vec{\tilde{H}}_{pilot},$$

and $Tr\{\bullet\}$ denotes the trace of matrix. R_{hh}, R_{hp} and R_{pp} are the channel correlation matrices obtained from the channel statistical information which are expressed as:

$$\begin{aligned} R_{hh} &= \mathbb{E}[\vec{H}\vec{H}^H] \\ R_{hp} &= \mathbb{E}[\vec{H}\vec{H}_p^H] \\ R_{pp} &= \mathbb{E}[\vec{H}_p\vec{H}_p^H] \end{aligned} \tag{28}$$

Based on (26) and (27), we can compare the MSE of the pilot-aided and data-aided estimation processes. As a result, we select the CFR with the lower MSE for equalization. We denote that $T = \frac{1}{N} Tr\{R_{hh} - 2Re[F_{in}R_{hp}^H] + F_{in}(R_{pp} + \frac{\sigma_w^2}{\sigma_x^2}\boldsymbol{I}_{N_p})F_{in}^H\}$. Due to the assumption of perfect detection, the selected CFR can be obtained as:

$$\vec{\tilde{H}}^{(i)} = \begin{cases} \dfrac{\vec{Y}_{data}(n)}{\vec{\tilde{X}}_{data}(n)} & \dfrac{\sigma_w^2}{|\vec{\tilde{X}}|^2} < T \\ \vec{\tilde{H}}^{(i-1)} & \dfrac{\sigma_w^2}{|\vec{\tilde{X}}|^2} > T \end{cases} \quad n = 0, 1, \cdots, N-1, \tag{29}$$

where i denotes the ith iteration and $\vec{\tilde{H}}^{(i-1)}$ is the CFR of the previous iteration. From (29), we define a threshold λ to simplify (29) which is given as:

$$\lambda = \sqrt{\frac{\sigma_w^2}{Z}} \tag{30}$$

We substitute (30) into (29), and then the threshold control at ith iteration can be rearranged as

$$\vec{\tilde{H}}^{(i)} = \begin{cases} \dfrac{\vec{Y}_{data}(n)}{\vec{\tilde{X}}_{data}(n)} & |\vec{\tilde{X}}_{data}(n)| > \lambda \\ \vec{\tilde{H}}^{(i-1)} & |\vec{\tilde{X}}_{data}(n)| \le \lambda \end{cases} \quad n = 0, 1, \cdots, N-1, \tag{31}$$

Combined with the threshold control strategy, the complete Turbo receiver channel estimation for GFDM-based CR networks is summarized in Table.1.

V. SIMULATION RESULTS AND DISCUSSIONS

In this section, we evaluate the performance of the proposed Turbo receiver channel estimation for GFDM-based CR networks. We adopt a $L = 24$ path frequency selective mulipath channel with Rayleigh distribution. The BER, Symbol Error Rate (SER) and MSE are selected as performance metrics. The simulation parameters are listed in Table. 2. The Monte-Carlo method is used for our simulation.

TABLE 1. Threshold control based Turbo receiver GFDM channel estimation algorithm.

Algorithm 1

Calculate pilot-aided initial channel estimation CFR $\vec{H}_p$, according to (20) and (21)
$\vec{H}_{ce} = \vec{H}_p$
for i = 0:Niter
  equalize the received signal with $\vec{H}_{ce}$, according to (10)
  demodulate and demap the equalized symbols, according to (13)
  decode the demapped data to get the likelihood ratio
  encode and map the soft information using (22), (23) and (24)
  rebuild the symbols $\vec{X}_d$
  calculate the data-aided channel estimation CFR $\vec{H}_d$ using (25)
  calculate the threshold λ according to (27) and (30)
  for n=0:N-1
    if $|\vec{X}_d(n)| > \lambda(n)$
      $\vec{H}_{ce}(n) = \vec{H}_d(n)$
    end
  end
end
calculate the final decoded bits by hard decision

TABLE 2. Simulation parameters.

Parameter	GFDM
Number of subcarriers	96
Number of subsymbols	7
Modulation mode	16-QAM
Pulse shaped filter	Raised-cosine filter
Roll-off factor	0.3
GFDM modulation	Frequency domain modulation
Pilot sequence	Complex random and Zadoff-Chu
Pilot spacing	4
Channel coding	Turbo coding
Generating matrix	(1,1,1,1;1,1,0,1)
Coding rate	5/6,1/3
GFDM demodulation	Zero Forcing
Channel equalization	MMSE
Component decoder	log-MAP
Number of decoder iteration	8

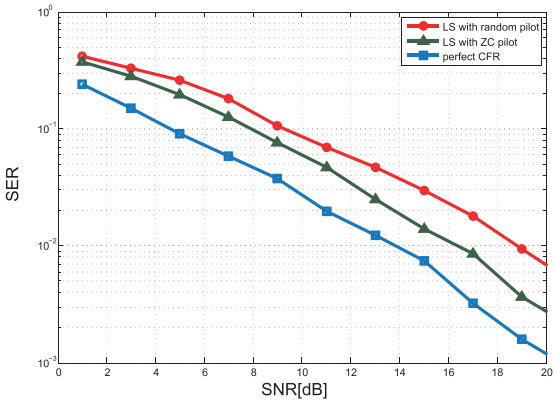

FIGURE 10. Symbol error rate performance with different pilots.

Fig. 10 shows the SER performance in the case without Turbo codes. We can see that due to the constant amplitude zero auto-correlation characteristic of Zadoff-Chu (ZC) sequence, the SER performance of the LS channel estimation which uses the ZC pilots is better than the LS channel estimation which uses complex random pilots. In the case of perfect CFR, the SER performance is the best.

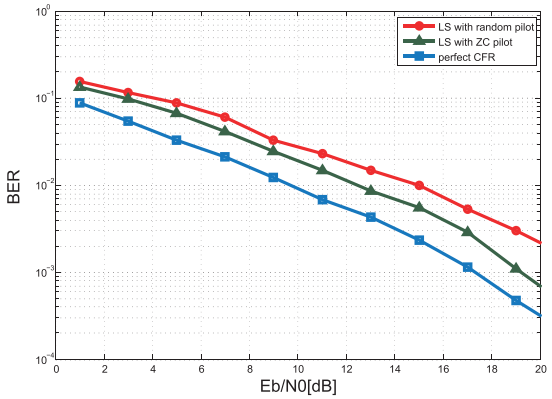

FIGURE 11. Bit error rate performance with 5/6 coding rate.

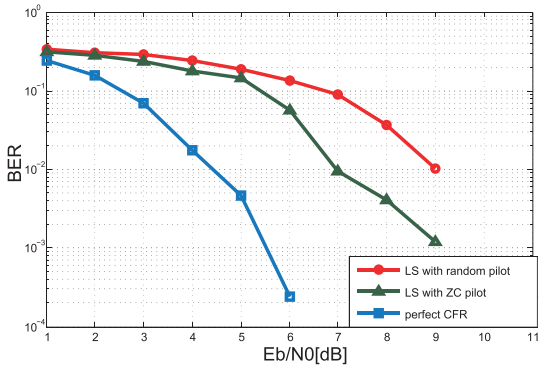

FIGURE 12. Bit error rate performance with 1/3 coding rate.

Fig. 11 and Fig. 12 demonstrate the BER performance of Turbo-coded channel estimation in different coding rates. By means of the Turbo-coded channel coding and Turbo receiver, the BER performance is improved compared with the case without Turbo codes. Fig. 11 presents the performance of coded GFDM system channel estimation with the coding rate of 5/6. We can see that even when the coding rate is high, the Turbo-coded GFDM system still has a considerable performance improvement compared with the uncoded system. We note that when $Eb/N0$ is about 10dB, the BER is still above 10^{-3}. When the coding rate is 1/3, the BER performance is provided in Fig. 12. When $Eb/N0$ is about 10dB, the BER performance is far below 10^{-3}. Using the perfect CFR, the bit error can be reduced to nearly zero at $Eb/N0 > 6$dB regions. Due to ZC pilots, the required $Eb/N0$ for BER $= 10^{-2}$ is reduced by 2dB compared with the LS estimation with complex random pilots.

The MSE performance of the basic LS and the Threshold Control (TC) based Turbo receiver channel estimation for GFDM is evaluated in Fig. 13. At the low $Eb/N0$ regions, with the increase of iterative number, the MSE performance is improved. The basic LS channel estimation is worse than the proposed TC-based Turbo receiver channel estimation. Because of the use of orthogonal pilots, the Turbo receiver channel estimation will be approximate to LS channel estimation at the high $Eb/N0$ regions.

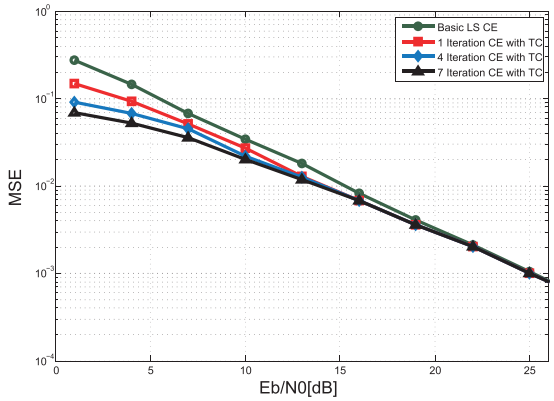

FIGURE 13. MSE performance of LS and threshold control iterative channel estimation with 1/3 coding rate.

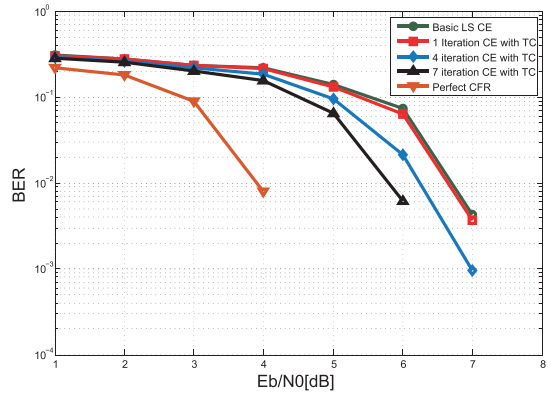

FIGURE 14. BER performance of LS and different iterative number channel estimation with 1/3 coding rate.

We can see from the Fig. 14 that the proposed TC-based Turbo receiver channel estimation in different numbers of iteration outperforms the basic LS channel estimation. With the increase of iteration number, the BER performance is gradually improved.

VI. CONCLUSIONS

In this paper, a Turbo receiver channel estimation for GFDM-based CR networks is proposed. The Turbo receiver is redesigned to achieve the data-aided iterative channel estimation in GFDM system. A threshold control strategy is proposed to rule out the unauthentic rebuilt symbols. Based on the proposed TC strategy, the noise enhancement is counteracted. The proposed channel estimation is verified by the simulation of the SER, BER and MSE performances. We observe that the basic LS channel estimation in Turbo-coded GFDM systems has the obvious improvement compared with the case without Turbo codes. When the coding rate decreases, the BER performance is enhanced at the cost of the lower spectrum efficiency. By using ZC sequence as the pilot sequence, the SER and BER performances are improved. The proposed Turbo receiver channel estimation has the better BER and MSE performance than the basic LS channel estimation. The BER and MSE performances can be improved with the increase of iterative times. We can select the appropriate iteration number to trade off the required performance and the computing overhead.

REFERENCES

[1] H. Men, N. Zhao, M. Jin, and J. M. Kim, "Optimal transceiver design for interference alignment based cognitive radio networks," *IEEE Commun. Lett.*, vol. 19, no. 8, pp. 1442–1445, Aug. 2015.
[2] I. Kakalou, K. E. Psannis, P. Krawiec, and R. Badea, "Cognitive radio network and network service chaining toward 5G: Challenges and requirements," *IEEE Commun. Mag.*, vol. 55, no. 11, pp. 145–151, Nov. 2017.
[3] X. Liu, F. Li, and Z. Na, "Optimal resource allocation in simultaneous cooperative spectrum sensing and energy harvesting for multichannel cognitive radio," *IEEE Access*, vol. 5, pp. 3801–3812, 2017.
[4] N. Zhao, F. R. Yu, H. Sun, and M. Li, "Adaptive power allocation schemes for spectrum sharing in interference-alignment-based cognitive radio networks," *IEEE Trans. Veh. Technol.*, vol. 65, no. 5, pp. 3700–3714, May 2016.
[5] X. Li, N. Zhao, Y. Sun, and F. R. Yu, "Interference alignment based on antenna selection with imperfect channel state information in cognitive radio networks," *IEEE Trans. Veh. Technol.*, vol. 65, no. 7, pp. 5497–5511, Jul. 2016.
[6] S. Li, M. Sun, Y.-C. Liang, B. Li, and C. Zhao, "Spectrum sensing for cognitive radios with unknown noise variance and time-variant fading channels," *IEEE Access*, vol. 5, pp. 21992–22003, 2017.
[7] Z. Hu, N. Wei, and Z. Zhang, "Optimal resource allocation for harvested energy maximization in wideband cognitive radio network with SWIPT," *IEEE Access*, vol. 5, pp. 23383–23394, 2017.
[8] Y. Wang, Y. Wang, F. Zhou, Y. Wu, and H. Zhou, "Resource allocation in wireless powered cognitive radio networks based on a practical non-linear energy harvesting model," *IEEE Access*, vol. 5, pp. 17618–17626, 2017.
[9] C. Qi, G. Yue, L. Wu, and A. Nallanathan, "Pilot design for sparse channel estimation in OFDM-based cognitive radio systems," *IEEE Trans. Veh. Technol.*, vol. 63, no. 2, pp. 982–987, Feb. 2014.
[10] N. Michailow *et al.*, "Generalized frequency division multiplexing for 5th generation cellular networks," *IEEE Trans. Commun.*, vol. 62, no. 9, pp. 3045–3061, Sep. 2014.
[11] J. Datta, H.-P. Lin, and D.-B. Lin, "Spatial modulation based location aware beam-forming in GFDM modulated cognitive radio systems," in *Proc. Int. Conf. Appl. Syst. Innov. (ICASI)*, May 2017, pp. 103–106.
[12] R. Datta, N. Michailow, S. Krone, M. Lentmaier, and G. Fettweis, "Generalized frequency division multiplexing in cognitive radio," in *Proc. 20th Eur. Signal Process. Conf. (EUSIPCO)*, Aug. 2012, pp. 2679–2683.
[13] H. Zhang, D. Le Ruyet, D. Roviras, and H. Sun, "Noncooperative multicell resource allocation of FBMC-based cognitive radio systems," *IEEE Trans. Veh. Technol.*, vol. 61, no. 2, pp. 799–811, Feb. 2012.
[14] Y. Medjahdi, M. Terre, D. Le Ruyet, D. Roviras, and A. Dziri, "Performance analysis in the downlink of asynchronous OFDM/FBMC based multi-cellular networks," *IEEE Trans. Wireless Commun.*, vol. 10, no. 8, pp. 2630–2639, Aug. 2011.
[15] B. Farhang-Boroujeny, "OFDM versus filter bank multicarrier," *IEEE Signal Process. Mag.*, vol. 28, no. 3, pp. 92–112, May 2011.
[16] T. Yunzheng, L. Long, L. Shang, and Z. Zhi, "A survey: Several technologies of non-orthogonal transmission for 5G," *China Commun.*, vol. 12, no. 10, pp. 1–15, Oct. 2015.
[17] D. Zhang, A. Festag, and G. P. Fettweis, "Performance of generalized frequency division multiplexing based physical layer in vehicular communications," *IEEE Trans. Veh. Technol.*, vol. 66, no. 11, pp. 9809–9824, Nov. 2017.
[18] M. Danneberg *et al.*, "Implementation of a 2 by 2 MIMO-GFDM transceiver for robust 5G networks," in *Proc. Int. Symp. Wireless Commun. Syst. (ISWCS)*, Aug. 2015, pp. 236–240.
[19] W. Zhang, F. Gao, and Q. Yin, "Blind channel estimation for MIMO-OFDM systems with low order signal constellation," *IEEE Commun. Lett.*, vol. 19, no. 3, pp. 499–502, Mar. 2015.
[20] Y. Liu, Z. Tan, H. Hu, L. J. Cimini, and G. Y. Li, "Channel estimation for OFDM," *IEEE Commun. Surveys Tuts.*, vol. 16, no. 4, pp. 1891–1908, 4th Quart., 2014.
[21] U. Vilaipornsawai and M. Jia, "Scattered-pilot channel estimation for GFDM," in *Proc. IEEE Wireless Commun. Netw. Conf. (WCNC)*, Apr. 2014, pp. 1053–1058.
[22] S. Ehsanfar, M. Matthe, D. Zhang, and G. Fettweis, "Theoretical analysis and CRLB evaluation for pilot-aided channel estimation in GFDM," in *Proc. IEEE Global Commun. Conf. (GLOBECOM)*, Dec. 2016, pp. 1–7.

[23] S. Ehsanfar, M. Matthe, D. Zhang, and G. Fettweis, "Interference-free pilots insertion for MIMO-GFDM channel estimation," in *Proc. IEEE Wireless Commun. Netw. Conf. (WCNC)*, Mar. 2017, pp. 1–6.
[24] C.-T. Lam, D. D. Falconer, and F. Danilo-Lemoine, "A low complexity frequency domain iterative decision-directed channel estimation technique for single-carrier systems," in *Proc. IEEE 65th Veh. Technol. Conf. (VTC-Spring)*, Apr. 2007, pp. 1966–1970.
[25] D. Kim, H. M. Kim, and G. H. Im, "Iterative channel estimation with frequency replacement for SC-FDMA systems," *IEEE Trans. Commun.*, vol. 60, no. 7, pp. 1877–1888, Jul. 2012.
[26] S. Park, B. Shim, and J. W. Choi, "Iterative channel estimation using virtual pilot signals for MIMO-OFDM systems," *IEEE Trans. Signal Process.*, vol. 63, no. 12, pp. 3032–3045, Jun. 2015.
[27] H.-M. Kim, D. Kim, T.-K. Kim, and G.-H. Im, "Frequency domain channel estimation for MIMO SC-FDMA systems with CDM pilots," *J. Commun. Netw.*, vol. 16, no. 4, pp. 447–457, Aug. 2014.
[28] O. O. Ogundile, O. O. Oyerinde, and D. J. J. Versfeld, "Decision directed iterative channel estimation and Reed–Solomon decoding over flat fading channels," *IET Commun.*, vol. 9, no. 17, pp. 2077–2084, 2015.
[29] D. Yoon and J. Moon, "Low-complexity iterative channel estimation for turbo receivers," *IEEE Trans. Commun.*, vol. 60, no. 5, pp. 1182–1187, May 2012.
[30] Q. Li, K. C. Teh, and K. H. Li, "Low-complexity channel estimation and turbo equalisation for high frequency channels," *IET Commun.*, vol. 7, no. 10, pp. 980–987, Jul. 2013.
[31] I. Gaspar, M. Matthé, N. Michailow, L. L. Mendes, D. Zhang, and G. Fettweis. (Jun. 2015). "GFDM transceiver using precoded data and low-complexity multiplication in time domain." [Online]. Available: https://arxiv.org/abs/1506.03350

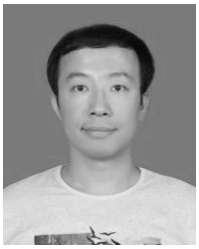

ZHENYU NA received the B.S. and M.S. degrees in communication engineering from the Harbin Institute of Technology, China, in 2004 and 2007, respectively, and the Ph.D. degree in information and communication engineering from the Communication Research Center, Harbin Institute of Technology, in 2010. He is currently an Associate Professor with the School of Information Science and Technology, Dalian Maritime University, China. His research interests include satellite communications and networking, OFDM, non-orthogonal multicarrier transmissions, NOMA, and wireless powered communication networks.

ZHENG PAN received the B.S. degree in communication engineering from Dalian Maritime University, Dalian, China, in 2014, where he is currently pursuing the M.S. degree with the School of Information Science and Technology. His research interests include 5G wireless communications, channel estimation, OFDM, NOMA, and satellite communication.

MUDI XIONG received the M.Sc. degree in physics electronics from the Changchun Institute of Optics and Fine Mechanics in 1994, and the Ph.D. degree in optical engineering from the Changchun Institute of Optics, Fine Mechanics and Physics, Chinese Academy of Sciences, in 2000. He was an Associate Professor with the Harbin Institute of Technology. In 2003, he joined Dalian Maritime University, where he has been the full-time Professor, Since 2006. His research field includes optical signal detection, optical communications, and networking.

XIN LIU received the M.Sc. and the Ph.D. degrees in communication engineering from the Harbin Institute of Technology in 2008 and 2012, respectively. From 2012 to 2013, he was a Research Fellow with the School of Electrical and Electronic Engineering, Nanyang Technological University, Singapore. From 2013 to 2016, he was a Lecturer with the College of Astronautics, Nanjing University of Aeronautics and Astronautics, China. He is currently an Associate Professor with the School of Information and Communication Engineering, Dalian University of Technology, China. His research interests focus on communication signal processing, cognitive radio, spectrum resource allocation, and broadband satellite communications.

WEIDANG LU (S'08–M'13) received the Ph.D. degree in information and communication engineering from the Harbin Institute of Technology in 2012. He was a Visiting Scholar with the Nanyang Technology University, Singapore, The Chinese University of Hong Kong, China, and the Southern University of Science and Technology, China. He is currently an Associate Professor with the College of Information Engineering, Zhejiang University of Technology, Hangzhou, China. His current research interests include simultaneous wireless information and power transfer, wireless sensor networks, cooperative communications, and physical layer security for wireless systems.

YONGJIAN WANG received the M.Sc. and Ph.D. degrees in communication engineering from the Harbin Institute of Technology, in 2008 and 2012, respectively. From 2006 to 2008, he was a Research Fellow with the Research Room on Communications, National Institute of Advanced Industrial Science and Technology, Japan. Since 2010, he has been an Associated Professor with the Laboratory of the National Computer Network Emergency Response Technical Team/Coordination Center of China (CNCERT/cc). He is currently an Associate Professor with CNCERT/cc. His research interests focus on communication signal processing, cognitive radio, 5G, and the security of IoT.

LISHENG FAN received the B.S. degree from the Department of Electronic Engineering, Fudan University, in 2002, and the M.S. degree from the Department of Electronic Engineering, Tsinghua University, China, in 2005, and the Ph.D. degree from the Department of Communications and Integrated Systems, Tokyo Institute of Technology, Japan, in 2008. He is currently a Professor with Guangzhou University. He has authored or co-authored many papers in international journals, such as the IEEE TRANSACTIONS ON WIRELESS COMMUNICATIONS, the IEEE TRANSACTIONS ON COMMUNICATIONS, the IEEE TRANSACTIONS ON INFORMATION THEORY, and papers in conferences, such as the IEEE ICC, the IEEE GLOBECOM, and the IEEE WCNC. His research interests are in the areas of wireless cooperative communications, physical-layer secure communications, interference modeling, and system performance evaluation. He has also served as a member of Technical Program Committees for the IEEE conferences, such as GLOBECOM, ICC, WCNC, and VTC. He is a Guest Editor of the *EURASIP Journal on Wireless Communications and Networking*, and served as the Chair of Wireless Communications and Networking Symposium for CHINACOM 2014.